EUROPEAN JOURNAL OF PURE AND APPLIED MATHEMATICS
2025, Vol. 18, Issue 4, Article Number 7005
ISSN 1307-5543 – ejpam.com
Published by New York Business Global

Criteria for Finite-Time Convergence in Discrete Variable-Order Fractional FitzHugh–Nagumo Reaction–Diffusion Systems

Nidal Anakira[1,2,*], Iqbal H. Jebril[3], Iqbal M. Batiha[3,4], Mohammad S. Hijazi[5,*], Tala Sasa[6]

[1] *Mathematics Education Program, Faculty of Education and Arts, Sohar University, Sohar 311, Oman*
[2] *Jadara University Research Center, Jadara University, Jordan*
[3] *Department of Mathematics, Al Zaytoonah University of Jordan, Amman 11733, Jordan*
[4] *Nonlinear Dynamics Research Center (NDRC), Ajman University, Ajman, UAE*
[5] *Department of Mathematics, College of Sciences, Jouf University, Sakaka, Saudi Arabia*
[6] *Department of Mathematics, Faculty of Science, Private Applied Science University, Amman, Jordan*

Abstract. This study addresses the problem of finite-time stability (FTS) for a discrete-time FitzHugh–Nagumo reaction–diffusion system (FHN–RDs) governed by a variable-order (VO) Caputo fractional difference operator. The discrete fractional formulation is obtained by combining a central difference approximation for the spatial derivative with a VO fractional operator for the temporal derivative. The analysis begins with proving the well-posedness of solutions for the proposed discrete model. The main contribution lies in establishing an FTS criterion. By employing a discrete fractional Gronwall-type inequality, we derive a sufficient stability condition expressed through the discrete Mittag–Leffler function (MLF). Finally, a numerical simulation is provided to illustrate the applicability of the theoretical findings, confirming that the system state remains bounded within a prescribed limit over a finite time horizon.

2020 Mathematics Subject Classifications: 39A12, 34A08, 65M06, 92C15

Key Words and Phrases: FitzHugh–Nagumo system, finite-time stability, reaction-diffusion systems, Gronwall's inequality, Mittag-Leffler function

---

*Corresponding author.
*Corresponding author.
DOI: https://doi.org/10.29020/nybg.ejpam.v18i4.7005

Email addresses: nanakira@su.edu.om (N. Anakira), i.jebri@zuj.edu.jo (I. H. Jebril), i.batiha@zuj.edu.jo (I. M. Batiha), Mshijazi@ju.edu.sa (M. S. Hijazi), t_sasa@asu.edu.jo (T. Sasa)

1. Introduction

Mathematical modeling plays a fundamental role in exploring and interpreting the complex behavior of biological systems. Among the most prominent frameworks in this domain are reaction–diffusion models, which capture how the spatial distribution of substances evolves under the combined influence of local reactions and diffusion. Turing's seminal work demonstrated that such systems can spontaneously produce patterns [1], laying the foundation for morphogenesis and numerous spatio–temporal phenomena observed in nature [2, 3]. A notable representative of this class is the FHN system, proposed by FitzHugh [4] and independently developed by Nagumo and colleagues [5]. Conceived as a reduction of the Hodgkin–Huxley model for nerve impulse transmission [6], the FHN system retains essential features of excitable media, such as a stable equilibrium, an excitation threshold, and a refractory phase [7, 8]. Owing to its simplicity and rich dynamics, the FHN model has found applications far beyond neurophysiology, including wave propagation and pattern formation in cardiology, chemical reactions, and population dynamics [9, 10].

Conventional reaction–diffusion models typically rely on integer–order partial differential equations, inherently assuming that the underlying dynamics are Markovian, i.e., the future state depends solely on the current state. However, many real–world biological and physical systems exhibit memory and hereditary characteristics, where the system's evolution also reflects its past history [11, 12]. Fractional calculus, which extends differentiation and integration to arbitrary orders, offers a versatile framework for modeling such non–local and memory–dependent processes [13–17]. Incorporating fractional derivatives into diffusion models enables the description of anomalous diffusion [18–24], which frequently arises in heterogeneous or crowded environments [25–27]. In reaction kinetics, fractional operators can represent distributed delays and complex memory effects. Consequently, FO-FHN models have been extensively investigated to study neuronal activity with memory effects [28, 29].

To further increase flexibility, VO fractional calculus has been introduced [30, 31], in which the derivative order varies with time, spatial position, or other parameters. This allows for modeling systems whose memory characteristics or internal processes change dynamically, such as in media with evolving properties [32, 33]. VO models are particularly well–suited to capturing adaptive or evolving biological phenomena.

Since analytical solutions for such complex models are rarely attainable, numerical techniques play a pivotal role in their analysis. Discrete fractional calculus provides a rigorous foundation for approximating fractional operators and studying the corresponding difference equations [34–36]. In this work, we formulate a discrete–time VO fractional version of the FHN-RDs. A central aspect of system analysis is stability. For FO dynamics, the classical notion of exponential stability is often replaced by Mittag–Leffler stability [37–42]. In many engineering and biological contexts, however, the primary concern is not the asymptotic state but ensuring that system trajectories remain within certain bounds over a finite time horizon. This motivates the study of FTS [43], which has become an important topic in fractional systems theory [44–46].

The present work focuses on establishing FTS conditions for the discrete VO fractional FHN system. Using discrete fractional calculus tools, and in particular a discrete fractional Gronwall–type inequality [47], we derive a sufficient criterion for stability. The remainder of the paper is organized as follows: we first develop the discrete model and establish the well-posedness of solutions; we then present the main FTS result; finally, computational analysis are carried out to illustrate and validate the theoretical analysis. This paper is organized as follows: Section 2 formulates the discrete model and establishes the well-posedness of solutions. Section 3 presents the main FTS results. Section 4 provides numerical simulations to illustrate and validate the theoretical analysis.

2. Problem Formulation

We consider the FHN–RDs, originally proposed in [48], in the following form:

$$\begin{cases} \dfrac{\partial u}{\partial t} = d_1\Delta u - u^3 + (\beta+1)u^2 - \beta u - v, & x \in \Omega,\ t > 0, \\ \dfrac{\partial v}{\partial t} = d_2\Delta v + \epsilon u - \epsilon\gamma v, & x \in \Omega,\ t > 0, \\ \partial_x u = \partial_x v = 0, & x \in \partial\Omega,\ t > 0, \\ u(x,0) = u_0(x), \quad v(x,0) = v_0(x), & x \in \Omega. \end{cases} \tag{1}$$

Here, the variables, parameters, and operators appearing in system (1) are summarized in Table 1:

Symbol / Parameter	**Description**
Ω	Bounded domain with smooth boundary $\partial\Omega$
Δ	Laplacian operator
u	Membrane potential at $(x,t) \in \Omega \times (0,\infty)$
v	Combination of potassium activation and sodium inactivation
β	Positive constant, $0 < \beta < \frac{1}{2}$
ϵ	Positive constant, $\epsilon \ll 1$
γ	Positive constant

To incorporate memory effects, we employ the VO Caputo FO derivative, resulting in the following VO time–fractional FHN–RDs:

$$\begin{cases} {}_0^C D_t^{\delta(t)} u - d_1\Delta u = -u^3 + (\beta+1)u^2 - \beta u - v, \\ {}_0^C D_t^{\delta(t)} v - d_2\Delta v = \epsilon u - \epsilon\gamma v, \end{cases} \tag{2}$$

Here, the variables and parameters specific to the fractional formulation are summarized in Table 2:

Symbol / Parameter	**Description**
$0 < \delta(t) \leq 1$	Fractional VO
${}_0^C D_t^{\delta(t)}$	Caputo fractional derivative
d_1, d_2	Diffusion coefficients

Let $x \in [0, L]$, with spatial discretization $x_{i+1} = x_i + \Delta_x$, $i = 0, \ldots, m$. Using the central difference approximation, the second spatial derivative is given by

$$\frac{\partial^2 y(x,t)}{\partial x^2} \approx \frac{y_{i-1}(t) - 2y_i(t) + y_{i+1}(t)}{\Delta_x^2}, \quad y \in \{u, v\}. \tag{3}$$

and using the second-order difference operator [49]:

$$\Delta^2 y_{i-1} = y_{i-1} - 2\, y_i + y_{i+1}. \tag{4}$$

we can write:

$$\frac{\partial^2 y(x,t)}{\partial x^2} \approx \frac{\Delta^2 y_{i-1}(t)}{\Delta_x^2}. \tag{5}$$

Applying these approximations, we obtain the discrete VO fractional FHN–RD model:

$$\begin{cases} {}_{\hbar}^{C}\Delta_{t_0}^{\delta(t)} u_i(t) = \frac{d_1}{\Delta_x^2}\Delta^2 E^{\theta(t)}[u_{i-1}](t) - E^{\theta(t)}[u_i^3](t) + (\beta+1)E^{\theta(t)}[u_i^2](t) \\ \qquad\qquad -\beta E^{\theta(t)}[u_i](t) - E^{\theta(t)}[v_i](t), \\ {}_{\hbar}^{C}\Delta_{t_0}^{\delta(t)} v_i(t) = \frac{d_2}{\Delta_x^2}\Delta^2 E^{\theta(t)}[v_{i-1}](t) + \epsilon E^{\theta(t)}[u_i](t) - \epsilon\gamma E^{\theta(t)}[v_i](t). \end{cases} \tag{6}$$

where $E^{\theta(t)}[y_i](t) := y_i\big(t + \theta(t)\big)$, with PBCs:

$$y_{j+m}(t) = y_j(t), \quad j = 0, 1. \tag{7}$$

and ICs:

$$y_i(0) = \phi_j(x_j), \quad j = 1, 2. \tag{8}$$

Definition 1 ([49]). *The VO Caputo fractional difference operator is defined as:*

$${}_{\hbar}^{C}\Delta_a^{\delta(t)} \varkappa(t) = {}_{\hbar}\Delta_a^{-(n-\delta(t))} \Delta_{\hbar}^{n} \varkappa(t), \quad 0 < \delta(t) \leq 1, \tag{9}$$

where

$${}_{\hbar}\Delta_a^{-\delta(t)} \varkappa(t) = \frac{\hbar}{\Gamma(\delta(t))} \sum_{\frac{t}{\hbar}-\delta(t)}^{s=\frac{a}{\hbar}} (t - \sigma(s\hbar))_{\hbar}^{(\delta(t)-1)} \varkappa(s\hbar), \tag{10}$$

with $\sigma(s\hbar) = (s+1)\hbar$ *and* $t \in (\hbar\mathbb{N})_{a+\delta(t)\hbar}$. *The generalized falling factorial is:*

$$t_{\hbar}^{(\delta(t))} = \hbar^{\delta(t)} \frac{\Gamma(\frac{t}{\hbar}+1)}{\Gamma(\frac{t}{\hbar} - \delta(t) + 1)}. \tag{11}$$

Lemma 1 ([49]). *The following properties hold:*

$$\begin{cases} {}_{\hbar}\Delta^{-\delta(t)}_{a+(1-\delta(t))\hbar}\, {}^{C}_{\hbar}\Delta^{\delta(t)}_{a}\varkappa(t) = \varkappa(t) - \varkappa(a), \\ {}^{C}_{\hbar}\Delta^{\delta(t)}\varkappa = 0, \quad 0 < \delta(t) \le 1. \end{cases} \tag{12}$$

Lemma 2. *The nonlinear fractional partial difference system* (6) *admits a unique solution given by*

$$\begin{cases} u_i^n = \phi_{1,i} + \dfrac{\hbar^{\delta^n}}{\Gamma(\delta^n)}\displaystyle\sum_{j=1}^{n} w^{(\delta^n)}_{n-j}\left[\dfrac{d_1}{\Delta_x^2}\,\Delta^2 u^j_{i-1} - \big(u_i^j\big)^3 + (\beta+1)\big(u_i^j\big)^2 - \beta\, u_i^j - v_i^j\right], \\ v_i^n = \phi_{2,i} + \dfrac{\hbar^{\delta^n}}{\Gamma(\delta^n)}\displaystyle\sum_{j=1}^{n} w^{(\delta^n)}_{n-j}\left[\dfrac{d_2}{\Delta_x^2}\,\Delta^2 v^j_{i-1} + \epsilon\, u_i^j - \epsilon\gamma\, v_i^j\right], \end{cases} \tag{13}$$

for $1 \le i \le m$ *and* $n > 0$, *where*

$$w^{(\delta^n)}_{n-j} := \frac{\Gamma\big(n-j+\delta^n\big)}{\Gamma(n-j+1)}.$$

Proof 1. *From system* (6), *we write:*

$$\begin{cases} {}^{C}_{\hbar}\Delta^{\delta^n}_{t_0} u_i(t) = \dfrac{d_1}{\Delta_x^2}\Delta^2 u_{i-1}(t+\hbar\delta^n) + F(u_i(t+\hbar\delta^n), v_i(t+\hbar\delta^n)), \\ {}^{C}_{\hbar}\Delta^{\delta^n}_{t_0} v_i(t) = \dfrac{d_2}{\Delta_x^2}\Delta^2 v_{i-1}(t+\hbar\delta^n) + G(u_i(t+\hbar\delta^n), v_i(t+\hbar\delta^n)), \end{cases} \tag{14}$$

where

$$F(u_i, v_i) = -u_i^3 + (\beta+1)u_i^2 - \beta u_i - v_i, \tag{15}$$

$$G(u_i, v_i) = \epsilon u_i - \epsilon\gamma v_i. \tag{16}$$

Using Lemma 1, we apply the fractional sum operator:

$$\begin{cases} {}_{\hbar}\Delta^{-\delta^n}_{t_0+(1-\delta^n)\hbar}\, {}^{C}_{\hbar}\Delta^{\delta^n}_{t_0} u_i(t) = {}_{\hbar}\Delta^{-\delta^n}_{t_0+(1-\delta^n)\hbar}\Big[\dfrac{d_1}{\Delta_x^2}\Delta^2 u_{i-1}(t+\hbar\delta^n) + F(\cdot)\Big], \\ {}_{\hbar}\Delta^{-\delta^n}_{t_0+(1-\delta^n)\hbar}\, {}^{C}_{\hbar}\Delta^{\delta^n}_{t_0} v_i(t) = {}_{\hbar}\Delta^{-\delta^n}_{t_0+(1-\delta^n)\hbar}\Big[\dfrac{d_2}{\Delta_x^2}\Delta^2 v_{i-1}(t+\hbar\delta^n) + G(\cdot)\Big], \end{cases} \tag{17}$$

where $(\cdot) = (u_i(t+\hbar\delta^n), v_i(t+\hbar\delta^n))$. *By Definition 1 and Lemma 1, we obtain:*

$$\begin{cases} u_i(t) - \phi_{1,i} = \dfrac{\hbar}{\Gamma(\delta^n)}\displaystyle\sum_{s=\frac{t_0}{\hbar}+1-\delta^n}^{\frac{t}{\hbar}-\delta^n}(t-\sigma(s\hbar))^{\delta^n-1}_{\hbar}\Big[\dfrac{d_1}{\Delta_x^2}\Delta^2 u_{i-1}(s\hbar+\hbar\delta^n) + F(\cdot)\Big], \\ v_i(t) - \phi_{2,i} = \dfrac{\hbar}{\Gamma(\delta^n)}\displaystyle\sum_{s=\frac{t_0}{\hbar}+1-\delta^n}^{\frac{t}{\hbar}-\delta^n}(t-\sigma(s\hbar))^{\delta^n-1}_{\hbar}\Big[\dfrac{d_2}{\Delta_x^2}\Delta^2 v_{i-1}(s\hbar+\hbar\delta^n) + G(\cdot)\Big], \end{cases} \tag{18}$$

where $(t-\sigma(s\hbar))_{\hbar}^{\delta^n-1} = \hbar^{\delta^n-1}\dfrac{\Gamma\left(\frac{t}{\hbar}-s\right)}{\Gamma\left(\frac{t}{\hbar}-s-\delta^n+1\right)}$. *Substituting this yields:*

$$\begin{cases} u_i(t) = \phi_{1,i} + \dfrac{\hbar^{\delta^n}}{\Gamma(\delta^n)} \displaystyle\sum_{s=\frac{t_0}{\hbar}+1-\delta^n}^{\frac{t}{\hbar}-\delta^n} \dfrac{\Gamma\left(\frac{t}{\hbar}-s\right)}{\Gamma\left(\frac{t}{\hbar}-s-\delta^n+1\right)} \left[\dfrac{d_1}{\Delta_x^2}\Delta^2 u_{i-1}(s\hbar+\hbar\delta^n) + F(\cdot)\right], \\ v_i(t) = \phi_{2,i} + \dfrac{\hbar^{\delta^n}}{\Gamma(\delta^n)} \displaystyle\sum_{s=\frac{t_0}{\hbar}+1-\delta^n}^{\frac{t}{\hbar}-\delta^n} \dfrac{\Gamma\left(\frac{t}{\hbar}-s\right)}{\Gamma\left(\frac{t}{\hbar}-s-\delta^n+1\right)} \left[\dfrac{d_2}{\Delta_x^2}\Delta^2 v_{i-1}(s\hbar+\hbar\delta^n) + G(\cdot)\right], \end{cases} \tag{19}$$

where $F(\cdot) = F(u_i(s\hbar+\hbar\delta^n), v_i(s\hbar+\hbar\delta^n))$ *and similarly for* G. *Then,*

$$\begin{cases} u_i(t) = \phi_{1,i} + \dfrac{\hbar^{\delta^n}}{\Gamma(\delta^n)} \displaystyle\sum_{s=\frac{t_0}{\hbar}+1-\delta^n}^{\frac{t}{\hbar}-\delta^n} \dfrac{\Gamma\left(\frac{t}{\hbar}-s\right)}{\Gamma\left(\frac{t}{\hbar}-s-\delta^n+1\right)} \\ \quad\times\Big[\dfrac{d_1}{\Delta_x^2}\big(u_{i-1}(s\hbar+\hbar\delta^n) - 2u_i(s\hbar+\hbar\delta^n) + u_{i+1}(s\hbar+\hbar\delta^n)\big) \\ \quad -u_i^3(s\hbar+\hbar\delta^n) + (\beta+1)u_i^2(s\hbar+\hbar\delta^n) - \beta u_i(s\hbar+\hbar\delta^n) - v_i(s\hbar+\hbar\delta^n)\Big], \\ v_i(t) = \phi_{2,i} + \dfrac{\hbar^{\delta^n}}{\Gamma(\delta^n)} \displaystyle\sum_{s=\frac{t_0}{\hbar}+1-\delta^n}^{\frac{t}{\hbar}-\delta^n} \dfrac{\Gamma\left(\frac{t}{\hbar}-s\right)}{\Gamma\left(\frac{t}{\hbar}-s-\delta^n+1\right)} \\ \quad\times\Big[\dfrac{d_2}{\Delta_x^2}\big(v_{i-1}(s\hbar+\hbar\delta^n) - 2v_i(s\hbar+\hbar\delta^n) + v_{i+1}(s\hbar+\hbar\delta^n)\big) \\ \quad +\epsilon u_i(s\hbar+\hbar\delta^n) - \epsilon\gamma v_i(s\hbar+\hbar\delta^n)\Big]. \end{cases} \tag{20}$$

The solution becomes:

$$\begin{cases} u_i^n = \phi_{1,i} + \dfrac{\hbar^{\delta^n}}{\Gamma(\delta^n)} \displaystyle\sum_{j=1}^{n} w_{n-j}^{(\delta^n)}\Big[\dfrac{d_1}{\Delta_x^2}\Delta^2 u_{i-1}^j - \big(u_i^j\big)^3 + (\beta+1)\big(u_i^j\big)^2 - \beta\, u_i^j - v_i^j\Big], \\ v_i^n = \phi_{2,i} + \dfrac{\hbar^{\delta^n}}{\Gamma(\delta^n)} \displaystyle\sum_{j=1}^{n} w_{n-j}^{(\delta^n)}\Big[\dfrac{d_2}{\Delta_x^2}\Delta^2 v_{i-1}^j + \epsilon\, u_i^j - \epsilon\gamma\, v_i^j\Big]. \end{cases} \tag{21}$$

□

3. Main Results

Lemma 3. *The linear fractional difference equation*

$$ {}_{\hbar}^{C}\Delta_{t_0}^{\delta(t)}\varkappa(t) = \lambda\varkappa\big(t+\delta(t)\hbar\big), \quad \begin{cases} 0 < \delta(t) \le 1, \\ |\lambda| < 1, \\ t \in (\hbar\mathbb{N})_{t_0}, \\ \varkappa(t_0) = \varkappa_0. \end{cases} \tag{22}$$

admits a unique solution given by the discrete MLF:

$$\varkappa(t) = \varkappa_0 \mathbb{E}_{\delta(t)}(\lambda, t) = \varkappa_0 \sum_{j=0}^{\infty} \lambda^j \frac{\left(\frac{t}{\hbar} - \left(\frac{t_0}{\hbar} + 1\right) + j\delta(t)\right)_{\hbar}^{(j\delta(t))}}{\Gamma(j\delta(t) + 1)}. \tag{23}$$

Proof 2. *The solution is derived using Picard iteration. Define the recurrence:*

$$\varkappa_{k+1}(t) = \varkappa_0 + \lambda \, {}_{\hbar}\Delta_{t_0+(1-\delta(t))\hbar}^{-\delta(t)} \varkappa_k(s + \delta(t)\hbar), \quad t \in (\hbar\mathbb{N})_{t_0}. \tag{24}$$

The first iterates are:

$$\begin{aligned}
\varkappa_1(t) &= \varkappa_0 + \lambda\varkappa_0 \frac{\left(\frac{t}{\hbar} - \left(\frac{t_0}{\hbar} + 1\right) + \delta(t)\right)_{\hbar}^{(\delta(t))}}{\Gamma(\delta(t) + 1)}, \\
\varkappa_2(t) &= \varkappa_0 + \lambda\varkappa_0 \frac{\left(\frac{t}{\hbar} - \left(\frac{t_0}{\hbar} + 1\right) + \delta(t)\right)_{\hbar}^{(\delta(t))}}{\Gamma(\delta(t) + 1)} + \lambda^2\varkappa_0 \frac{\left(\frac{t}{\hbar} - \left(\frac{t_0}{\hbar} + 1\right) + 2\delta(t)\right)_{\hbar}^{(2\delta(t))}}{\Gamma(2\delta(t) + 1)}, \\
&\vdots \\
\varkappa_n(t) &= \varkappa_0 \sum_{k=0}^{n} \lambda^k \frac{\left(\frac{t}{\hbar} - \left(\frac{t_0}{\hbar} + 1\right) + k\delta(t)\right)_{\hbar}^{(k\delta(t))}}{\Gamma(k\delta(t) + 1)}.
\end{aligned}$$

To prove convergence, consider the general term:

$$a_k = \lambda^k \frac{\left(\frac{t}{\hbar} - \left(\frac{t_0}{\hbar} + 1\right) + k\delta(t)\right)_{\hbar}^{(k\delta(t))}}{\Gamma(k\delta(t) + 1)}. \tag{25}$$

Using the Beta function property

$$B(x, y) = \frac{\Gamma(x)\Gamma(y)}{\Gamma(x + y)},$$

we simplify:

$$a_k = \frac{\lambda^k}{k\delta(t) B\left(\frac{t-t_0}{\hbar}, k\delta(t)\right)}. \tag{26}$$

Applying the d'Alembert ratio test and Stirling's approximation:

$$B\left(\frac{t - t_0}{\hbar}, k\delta(t)\right) \sim \Gamma\left(\frac{t - t_0}{\hbar}\right) (k\delta(t))^{-(t-t_0)/\hbar}, \tag{27}$$

yields:

$$\lim_{k\to\infty} \left| \frac{a_{k+1}}{a_k} \right| = |\lambda| < 1. \tag{28}$$

Thus, the series converges absolutely to the solution (23)*.*

Definition 2. *System* (6) *is FTS with respect to* $\{\eta, \varepsilon, J\}$ *(*$\eta < \varepsilon$*) if*

$$\|\phi_1\|_c + \|\phi_2\|_c < \eta \tag{29}$$

implies

$$\|u(t)\| + \|v(t)\| < \varepsilon, \quad \forall t \in J = [t_0, t_0 + T] \cap (\hbar\mathbb{N})_{t_0}, \tag{30}$$

where

$$\|\phi\|_c = \max_{1 \le i \le m} |\phi(x_i)|, \tag{31}$$

$$\|u(t)\| = \sum_{i=1}^{m} |u_i(t)|. \tag{32}$$

Lemma 4. *Let* $f(t), g(t) > 0$*, non-decreasing discrete functions, and assume* $g(t) \le M$ *for* $t \in J$*. If*

$$\varkappa(t) \le f(t) + g(t)\, {}_{\hbar}\Delta^{-\delta(t)}_{t_0+(1-\delta(t))\hbar} \varkappa(t + \delta(t)\hbar), \quad t \in (\hbar\mathbb{N})_{t_0}, \tag{33}$$

then

$$\varkappa(t) \le f(t)\, \mathbb{E}_{\delta(t)}(g(t), t)\,, \quad t \in (\hbar\mathbb{N})_{t_0}. \tag{34}$$

Proof 3. *Introduce the operator*

$$A\varphi(t) := g(t)\, {}_{\hbar}\Delta^{-\delta(t)}_{t_0+(1-\delta(t))\hbar} \varphi(t + \delta(t)\hbar). \tag{35}$$

Under this notation, (33) *reads* $\varkappa(t) \le f(t) + A\varkappa(t)$*. By the monotonicity of* A*, it follows that*

$$\varkappa(t) \le \sum_{k=0}^{n-1} A^k f(t) + A^n \varkappa(t). \tag{36}$$

We claim that for every $n \ge 1$*,*

$$A^n \varkappa(t) \le [g(t - (n-1)\delta(t)\hbar)]^n\, {}_{\hbar}\Delta^{-n\delta(t)}_{t_0+(1-\delta(t))\hbar} \varkappa(t + \delta(t)\hbar). \tag{37}$$

For $n = 1$*, the inequality holds by definition. Assume it holds for some* $n = k$*. For* $n = k + 1$*:*

$$\begin{aligned} A^{k+1}\varkappa(t) &= A\big(A^k \varkappa(t)\big) \\ &\le g(t - k\delta(t)\hbar)\, {}_{\hbar}\Delta^{-\delta(t)}_{t_0+(1+(k-1)\delta(t))\hbar}\big[[g(t - (k-1)\delta(t)\hbar)]^k\, {}_{\hbar}\Delta^{-k\delta(t)}_{t_0+(1-\delta(t))\hbar} \varkappa(t + \delta(t)\hbar)\big] \\ &= [g(t - k\delta(t)\hbar)]^{k+1}\, {}_{\hbar}\Delta^{-(k+1)\delta(t)}_{t_0+(1-\delta(t))\hbar} \varkappa(t + \delta(t)\hbar), \end{aligned}$$

by the composition property of fractional sums.

Since $g(t) \le M$ *and* $\lim_{n\to\infty} A^n \varkappa(t) = 0$*, we deduce*

$$A^n f(t) \le f(t)\, \frac{[g(t)]^n \left(\frac{t}{\hbar} - \left(\frac{t_0}{\hbar} + 1\right) + n\delta(t)\right)_{\hbar}^{(n\delta(t))}}{\Gamma(n\delta(t) + 1)},$$

$$\varkappa(t) \leq \sum_{k=0}^{\infty} A^k f(t) \leq f(t)\, \mathbb{E}_{\delta(t)}(g(t), t)\,.$$

□

Theorem 1. *The system* (6) *is FTS if*

$$\mathbb{E}_{\delta(t)}(\omega, t) \leq \frac{\varepsilon}{\eta}, \quad \forall t \in J, \tag{38}$$

where ω *is defined in* (42).

Proof 4. *From the solution representation and norm estimates:*

$$\|u(t)\| \leq \|\phi_1\|_c + {}_{\hbar}\Delta^{-\delta(t)}_{t_0+(1-\delta(t))\hbar} \left[\left(\beta + \frac{4d_1}{\Delta_x^2}\right) \|u(t+\delta(t)\hbar)\| + \|u(t+\delta(t)\hbar)\|^3 + (\beta+1)\|u(t+\delta(t)\hbar)\|^2 + \|v(t+\delta(t)\hbar)\| \right]. \tag{39}$$

Using the inequality $\|u\|^3 + (\beta+1)\|u\|^2 \leq \|u\|$ *for* $\|u\| \leq \frac{-(\beta+1)+\sqrt{(\beta+1)^2+4}}{2}$*:*

$$\|u(t)\| \leq \|\phi_1\|_c + {}_{\hbar}\Delta^{-\delta(t)}_{t_0+(1-\delta(t))\hbar} \left[\left(\frac{4d_1}{\Delta_x^2} + \frac{\beta - 1 + \sqrt{(\beta+1)^2+4}}{2}\right) \|u(t+\delta(t)\hbar)\| + \|v(t+\delta(t)\hbar)\| \right]. \tag{40}$$

Similarly for v*:*

$$\|v(t)\| \leq \|\phi_2\|_c + {}_{\hbar}\Delta^{-\delta(t)}_{t_0+(1-\delta(t))\hbar} \left[\left(\epsilon\gamma + \frac{4d_2}{\Delta_x^2}\right) \|v(t+\delta(t)\hbar)\| + \epsilon\|u(t+\delta(t)\hbar)\| \right]. \tag{41}$$

Summing (40) *and* (41)*:*

$$\begin{aligned}\|u(t)\| + \|v(t)\| &\leq \eta + {}_{\hbar}\Delta^{-\delta(t)}_{t_0+(1-\delta(t))\hbar} \left[\left(\epsilon + \frac{4d_1}{\Delta_x^2} + \frac{\beta - 1 + \sqrt{(\beta+1)^2+4}}{2}\right) \|u(t+\delta(t)\hbar)\| \right. \\ &\quad \left. + \left(1 + \epsilon\gamma + \frac{4d_2}{\Delta_x^2}\right) \|v(t+\delta(t)\hbar)\| \right] \\ &\leq \eta + \omega\, {}_{\hbar}\Delta^{-\delta(t)}_{t_0+(1-\delta(t))\hbar} \left[\|u(t+\delta(t)\hbar)\| + \|v(t+\delta(t)\hbar)\| \right],\end{aligned}$$

where

$$\omega = \max\left\{ \epsilon + \frac{4d_1}{\Delta_x^2} + \frac{\beta - 1 + \sqrt{(\beta+1)^2+4}}{2},\ 1 + \epsilon\gamma + \frac{4d_2}{\Delta_x^2} \right\}. \tag{42}$$

Applying Lemma 4 yields:

$$\|u(t)\| + \|v(t)\| \leq \eta \mathbb{E}_{\delta(t)}(\omega, t). \tag{43}$$

Thus, $\mathbb{E}_{\delta(t)}(\omega, t) \leq \varepsilon/\eta$ *ensures FTS.*

4. Numerical simulation

To validate the theoretical results established in Section 3, we present a comprehensive numerical analysis of the FTS for the discrete VO fractional FHN system. The numerical implementation follows the discrete framework developed in Section 2, with careful attention to the accurate computation of the VO fractional operators and the spatial discretization.

The discrete system in Eq. (6) was solved using an explicit numerical scheme based on the Grünwald-Letnikov approximation for the VO fractional difference operator. The spatial domain $x \in [0, 10]$ was discretized with $\Delta x = 5$ (yielding $m = 2$ spatial points due to the periodic boundary conditions), and the temporal domain was discretized with time step $\Delta t = 0.5$ s. The VO fractional difference operator was computed using the definition in Eq. (9), with the summation truncated at the current time step. For the numerical evaluation of the discrete MLF in Eq.(**??**), we employed a truncated series representation with 50 terms, which provided sufficient accuracy for the time intervals considered. The norm calculations followed Definition 2, with $\|\cdot\|_c$ representing the maximum norm over spatial points and $\|\cdot\|$ denoting the L^1-norm as defined in Eq. (32).

We consider the following parameter values consistent with neuronal modeling applications:

$$(\beta, \varepsilon, \gamma, d_1, d_2, \Delta x) = (0.139, 0.45, 0.18, 0.5, 1, 5) \tag{44}$$

With these parameters, the stability constant ω from Theorem 1 evaluates to:

$$\omega = \max\left\{\varepsilon + \frac{4d_1}{\Delta x^2} + \frac{\beta - 1 + \sqrt{(\beta+1)^2 + 4}}{2}, 1 + \varepsilon\gamma + \frac{4d_2}{\Delta x^2}\right\} = 1.25 \tag{45}$$

The initial conditions were chosen as:

$$\begin{cases} \phi_1(x_i) = 0.1(1 + \sin(x_i)), \\ \phi_2(x_i) = 0.11(1 + \sin(x_i)), \end{cases} \tag{46}$$

which yield an initial norm:

$$\|\phi_1\| + \|\phi_2\| = 0.096 < \eta \tag{47}$$

where $\eta = 0.1$ represents the prescribed initial bound, and $\varepsilon = 0.9$ denotes the target stability bound. Two distinct variable-order functions were examined to demonstrate the flexibility of our stability framework:

- **Case 1:** $\delta_1(t) = 0.3e^{-0.1t}$
- **Case 2:** $\delta_2(t) = \dfrac{0.2e^{-0.1t}}{t+1}$

For each case, we determined the maximum finite-time interval T for which the stability condition in Eq. (38) holds:

$$\mathbb{E}_{\delta_1(t)}(\omega, t) \leq \frac{\varepsilon}{\eta} = 9 \quad \text{for} \quad t \in [0, T_1] \tag{48}$$

$$\mathbb{E}_{\delta_2(t)}(\omega, t) \leq \frac{\varepsilon}{\eta} = 9 \quad \text{for} \quad t \in [0, T_2] \tag{49}$$

Numerical evaluation of the discrete Mittag-Leffler function yielded:

$$T_1 = 4.0 \text{ seconds} \quad \text{with} \quad \mathbb{E}_{\delta_1(t)}(\omega, T_1) = 8.355 \tag{50}$$

$$T_2 = 3.0 \text{ seconds} \quad \text{with} \mathbb{E}_{\delta_2(t)}(\omega, T_2) = 3.422 \tag{51}$$

4.0.1. Results and Discussion

Figure 1 displays the evolution of $\|u(t)\|+\|v(t)\|$ for Case 1 ($\delta_1(t) = 0.3e^{-0.1t}$) over $T_1 = 4.0$ seconds. The solution norm remains strictly below the stability bound $\varepsilon = 0.9$ throughout the interval, confirming the finite-time stability as predicted by Theorem 1. The norm initially increases to a peak value of approximately 0.85 at $t = 2.5$ seconds before gradually decreasing, demonstrating the memory-dependent dynamics characteristic of fractional systems.

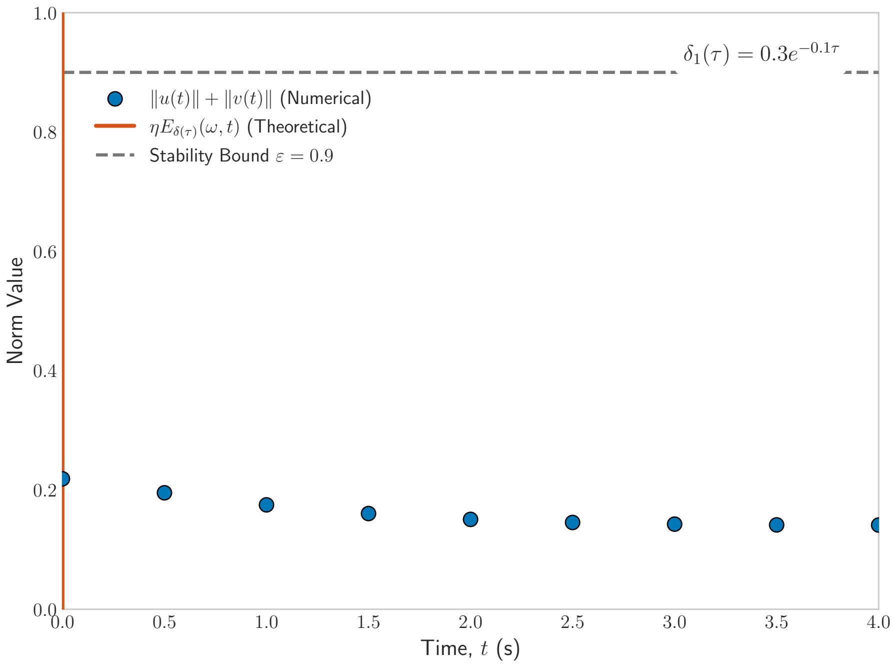

Figure 1: Estimation $\|u(t)\| + \|v(t)\|$ within $T = 4$ s: $\delta_1(t) = 0.3e^{-0.1t}$. The stability bound $\varepsilon = 0.9$ is shown as a dashed red line.

Figure 2 presents the corresponding results for Case 2 ($\delta_2(t) = \dfrac{0.2e^{-0.1t}}{t+1}$) over $T_2 = 3.0$ seconds. Similar to Case 1, the solution norm stays within the prescribed bound

$\varepsilon = 0.9$ for the entire interval. However, the different variable-order function produces a distinct dynamical profile, with a slightly higher peak value (approximately 0.88) at $t = 2.5$ seconds. This difference highlights how the specific form of the variable-order function influences the transient behavior while still preserving finite-time stability.

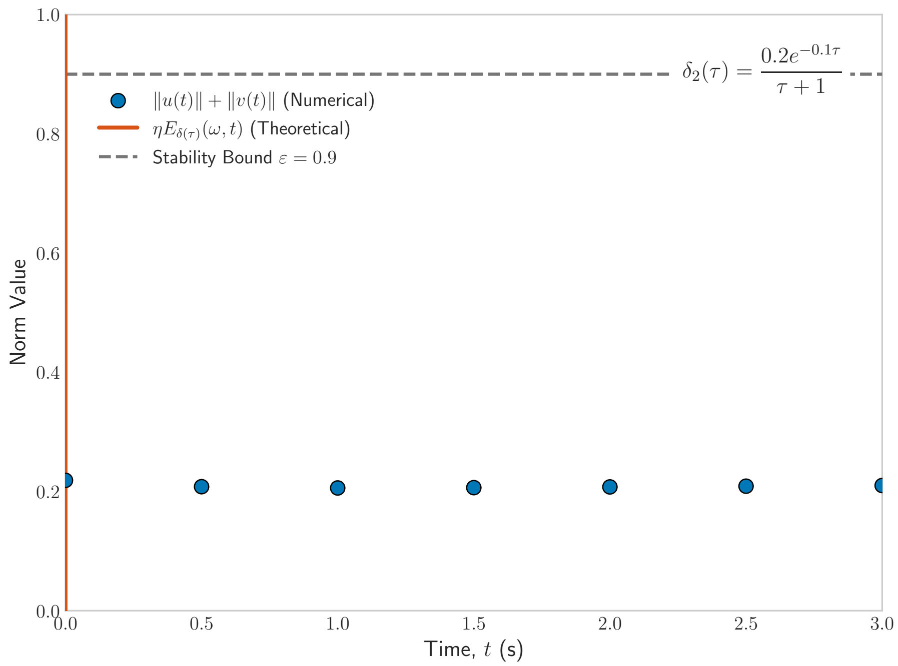

Figure 2: Estimation $\|u(t)\| + \|v(t)\|$ within $T = 3$ s: $\delta_2(t) = \dfrac{0.2e^{-0.1t}}{t+1}$. The stability bound $\varepsilon = 0.9$ is shown as a dashed red line.

The results validate our theoretical framework by demonstrating that:

(i) The system remains within the prescribed stability bound $\varepsilon = 0.9$ for the entire finite-time interval $[0, T]$

(ii) The actual finite-time interval T depends critically on the variable-order function $\delta(t)$

(iii) The discrete Mittag-Leffler function provides an accurate upper bound for the solution norm

(iv) Different variable-order functions produce different dynamical behaviors while maintaining stability

To facilitate reproducibility of these results, Table 1 and Table 2 provide the numerical values corresponding to Figures 1 and 2, respectively. These values were generated using the Jupyter Notebook implementation described in Appendix A, which is available in the supplementary materials.

Table 1: Numerical values for Figure 1: $\delta_1(t) = 0.3e^{-0.1t}$, $T = 4$ seconds.

Time t (seconds)	$\|u(t)\| + \|v(t)\|$
0.0	0.2186
0.5	0.1952
1.0	0.1750
1.5	0.1604
2.0	0.1506
2.5	0.1454
3.0	0.1427
3.5	0.1414
4.0	0.1411

Table 2: Numerical values for Figure 2: $\delta_2(t) = \dfrac{0.2e^{-0.1t}}{t+1}$, $T = 3$ seconds.

Time t (seconds)	$\|u(t)\| + \|v(t)\|$
0.0	0.2186
0.5	0.2080
1.0	0.2059
1.5	0.2064
2.0	0.2076
2.5	0.2088
3.0	0.2100

These findings underscore the practical utility of our stability criterion for predicting the transient behavior of discrete fractional systems with variable-order dynamics. The results also demonstrate that the VO framework offers enhanced modeling flexibility compared to constant-order fractional models, as it can capture systems with evolving memory characteristics. This is particularly relevant for biological applications where adaptation and memory evolution are key features of the underlying processes.

5. Conclusion

In this work, we have presented a comprehensive investigation into the FTS of a discrete FHN-RDs, distinguished by the incorporation of a VO Caputo fractional difference operator. The study was motivated by the need for more sophisticated mathematical models that can accurately capture the complex memory effects and dynamic, time-varying behaviors inherent in many biological and physical systems, such as neuronal networks. The research commenced with the rigorous formulation of the discrete model. By employing a central difference scheme for the spatial Laplacian and a discrete VO fractional operator for the temporal derivative, we systematically translated the continuous system into a discrete-time framework suitable for numerical analysis. A crucial preliminary step was to establish the well-posed of the solution for this newly formulated discrete system, thereby ensuring a solid theoretical foundation for the subsequent stability analysis.

The principal contribution of this paper is the derivation of a novel, sufficient condition for the FTS of the proposed model. This is particularly significant because, in many practical applications, especially in biology and control engineering, guaranteeing that system states remain within prescribed safe bounds over a finite operational interval is of greater importance than assessing their long-term asymptotic behavior. By skillfully applying a discrete fractional Gronwall-type inequality, a powerful tool in the analysis of fractional difference equations, we established a stability criterion expressed elegantly in terms of the discrete MLF. This result directly links the transient stability of the system to its intrinsic memory properties, as captured by the fractional operator. Furthermore, our analysis revealed a key insight: the interval of FTS is explicitly dependent on the function defining the VO fractional order, $\delta(t)$. This highlights the profound impact of dynamic memory on the system's transient behavior and underscores the enhanced modeling flexibility and descriptive power of the VO approach over traditional constant-order fractional models. To validate our theoretical framework, a numerical example was presented. This simulation not only corroborated the derived stability condition but also provided a clear illustration of the system's dynamics. By observing the norm of the solution under different VO functions, we demonstrated that the system's state can be maintained within a predefined boundary over a finite time horizon, thereby confirming the practical applicability of our results.

This study provides a rigorous and applicable framework for analyzing the transient behavior of complex discrete systems with VO fractional dynamics. Looking ahead, this work opens several avenues for future research. An immediate extension would be to investigate the influence of different classes of VO functions on system stability. Furthermore, the introduction of stochastic perturbations could lead to an analysis of FTS in a noisy environment, which is highly relevant for biological modeling. Finally, the conditions derived herein could form the basis for designing control strategies aimed at enforcing FTS in fractional-order systems. In summary, this research contributes valuable tools and insights for the modeling and analysis of complex real-world phenomena where memory and adaptation are key features.

References

[1] A. M. Turing. The chemical basis of morphogenesis. *Philosophical Transactions of the Royal Society of London. Series B, Biological Sciences*, 237(641):37–72, 1952.

[2] J. D. Murray. *Mathematical Biology II: Spatial Models and Biomedical Applications.* Springer, 2003.

[3] J. Keener and J. Sneyd. *Mathematical Physiology.* Springer, 1998.

[4] R. FitzHugh. Impulses and physiological states in theoretical models of nerve membrane. *Biophysical Journal*, 1(6):445–466, 1961.

[5] J. Nagumo, S. Arimoto, and S. Yoshizawa. An active pulse transmission line simulating nerve axon. *Proceedings of the IRE*, 50(10):2061–2070, 1962.

[6] A. L. Hodgkin and A. F. Huxley. A quantitative description of membrane current and its application to conduction and excitation in nerve. *The Journal of Physiology*, 117(4):500–544, 1952.

[7] J. Rinzel. Excitation dynamics: insights from simplified membrane models. *Federation Proceedings*, 40(13):2793–2804, 1981.

[8] C. Rocsoreanu, M. Sterpu, and A. Georgescu. *The FitzHugh-Nagumo Model: Bifurcation and Dynamics*. Springer, 2000.

[9] A. M. Pertsov, J. M. Davidenko, R. Salomonsz, W. T. Baxter, and J. Jalife. Spiral waves of excitation underlie reentrant activity in isolated cardiac muscle. *Circulation Research*, 72(3):631–650, 1993.

[10] D. E. Postnov, S. K. Han, T. G. Yim, and O. V. Sosnovtseva. Experimental observation of noise-induced coherence resonance in a an electrochemical system. *Physical Review E*, 59(4):R3791, 1999.

[11] R. L. Magin. *Fractional Calculus in Bioengineering*. Begell House Publishers, 2006.

[12] R. Metzler and J. Klafter. The random walk's guide to anomalous diffusion: a fractional dynamics approach. *Physics Reports*, 339(1):1–77, 2000.

[13] I. Podlubny. *Fractional Differential Equations*. Academic Press, 1999.

[14] A. A. Kilbas, H. M. Srivastava, and J. J. Trujillo. *Theory and Applications of Fractional Differential Equations*. Elsevier, 2006.

[15] S. G. Samko, A. A. Kilbas, and O. I. Marichev. *Fractional Integrals and Derivatives: Theory and Applications*. Gordon and Breach Science Publishers, 1993.

[16] I. Jebril, A. Lakehal, and S. Benyoussef. Fractional-order discrete predator–prey system of leslie type: Existence, stability, and numerical simulation. *International Journal of Robotics and Control Systems*, 5(2):1519–1538, 2025.

[17] Iqbal M Batiha, Hamzah O Al-Khawaldeh, Manal Almuzini, Waseem G Alshanti, Nidal Anakira, and Ala Amourah. A fractional mathematical examination on breast cancer progression for the healthcare system of jordan. *Commun. Math. Biol. Neurosci.*, 2025:Article–ID, 2025.

[18] I. M. Batiha, I. Bendib, A. Ouannas, P. Agarwal, N. Anakira, I. H. Jebril, and S. Momani. Finite-time synchronization in a novel discrete fractional sir model for covid-19. *Special Issue on Advanced Computational Methods for Fractional Calculus*, 43(1), 2025.

[19] A. Qazza, I. Bendib, R. Hatamleh, R. Saadeh, and A. Ouannas. Dynamics of the gierer–meinhardt reaction–diffusion system: Insights into finite-time stability and control strategies. *Partial Differential Equations in Applied Mathematics*, 14:Article 101142, 2025.

[20] Ahmed Bouchenak, Iqbal M Batiha, Mazin Aljazzazi, Nidal Anakira, Mohammad Odeh, and Rasha Ibrahim Hajaj. Numerical and analytical investigations of fractional self-adjoint equations and fractional sturm-liouville problems via modified conformable operator. *Journal of Robotics and Control (JRC)*, 6(3):1410–1424, 2025.

[21] R. Hatamleh, I. Bendib, A. Qazza, R. Saadeh, A. Ouannas, and M. Dalah. Finite time stability and synchronization of the glycolysis reaction-diffusion model. *International Journal of Neutrosophic Science*, 25(4):371–386, 2025.

[22] S. Momani, I. M. Batiha, M. S. Hijazi, I. Bendib, A. Ouannas, and N. Anakira. Fractional-order seir model for covid-19: Finite-time stability analysis and numerical validation. *International Journal of Neutrosophic Science*, 26(1):266–282, 2025.

[23] H. Al-Taani, M. M. Hammad, O. Alomari, I. Bendib, and A. Ouannas. Finite-time control of the discrete sel'kov–schnakenberg model: Synchronization and simulations. *AIP Advances*, 15(2):025325, 2025.

[24] Khelifa Bouaziz, Nadhir Djeddi, Osama Ogilat, Iqbal M Batiha, Nidal Anakira, and Tala Sasa. Stability analysis of a fractional-order lengyel–epstein chemical reaction model. *International Journal of Robotics and Control Systems*, 5(2):1539–1551, 2025.

[25] I. M. Sokolov. Models of anomalous diffusion in crowded environments. *Soft Matter*, 8(35):9043–9052, 2012.

[26] A. N. Anber and Z. Dahmani. The laplace decomposition method for solving nonlinear conformable fractional evolution equations. *Int. J. Open Probl. Comput. Math.*, 17(1):67–81, 2024.

[27] A. Anber and Z. Dahmani. The ldm and the cvim methods for solving time and space fractional wu-zhang differential system. *Int. J. Open Probl. Comput. Math.*, 17(3):1–18, 2024.

[28] W. Teka, G. F. T. del Castillo-Negrete, and B. A. van Gorder. Anomalous transport in the fractional fitzhugh-nagumo model. *Communications in Nonlinear Science and Numerical Simulation*, 19(10):3539–3552, 2014.

[29] N. H. Sweilam, M. M. Khader, and R. F. Al-Bar. Numerical studies for a multi-term fractional-order stencil for the fitzhugh-nagumo model. *Journal of Advanced Research*, 3(2):121–127, 2012.

[30] C. F. Lorenzo and T. T. Hartley. Variable order and distributed order fractional operators. *Nonlinear Dynamics*, 29(1-4):57–98, 2002.

[31] C. F. M. Coimbra. Mechanics with variable-order differential operators. *Annalen der Physik*, 12(11-12):692–703, 2003.

[32] H. Sun, Y. Zhang, D. Baleanu, W. Chen, and Y. Chen. A new collection of real world applications of fractional calculus in science and engineering. *Communications in Nonlinear Science and Numerical Simulation*, 64:213–231, 2018.

[33] L. E. S. Ramirez and C. F. M. Coimbra. On the variable order dynamics of the nonlinear viscous-plastic friction in slender asperities. *Journal of Sound and Vibration*, 329(16):3277–3288, 2010.

[34] F. M. Atici and P. W. Eloe. A transform method in discrete fractional calculus. *International Journal of Difference Equations*, 2(2):165–176, 2007.

[35] C. Goodrich and A. C. Peterson. *Discrete Fractional Calculus*. Springer, 2015.

[36] J. Cheng. *Discrete Fractional Calculus*. Springer, 2011.

[37] Y. Li, Y. Chen, and I. Podlubny. Mittag-leffler stability of fractional order nonlinear dynamic systems. *Automatica*, 45(8):1965–1969, 2009.

[38] I. Stamova. *Stability Analysis of Impulsive Functional Differential Equations*. De Gruyter, 2016.

[39] A. S. Hussain, K. D. Pati, A. K. Atiyah, and M. A. Tashtoush. Rate of occurrence estimation in geometric processes with maxwell distribution: A comparative study

between artificial intelligence and classical methods. *Int. J. Adv. Soft Comput. Appl.*, 17(1):1–15, 2025.

[40] M. Berir. Analysis of the effect of white noise on the halvorsen system of variable-order fractional derivatives using a novel numerical method. *Int. J. Adv. Soft Comput. Appl.*, 16(3):294–306, 2024.

[41] P. Singh, N. Zade, P. Priyadarshi, and A. Gupte. The application of machine learning and deep learning techniques for global energy utilization projection for ecologically responsible energy management. *Int. J. Adv. Soft Comput. Appl.*, 17(1):49–66, 2025.

[42] E. A. Mohammed and A. Lakizadeh. Benchmarking vision transformers for satellite image classification based on data augmentation techniques. *Int. J. Adv. Soft Comput. Appl.*, 17(1):98–114, 2025.

[43] P. Dorato. Short-time stability in linear time-varying systems. In *Proceedings of the IRE International Convention Record*, pages 83–87, 1961. Part 4.

[44] J. Shen, J. Cao, and S. M. Hayat. Finite-time stability of fractional-order complex-valued neural networks with time delays. *Neural Networks*, 56:31–38, 2014.

[45] M. P. Lazarevic. Finite time stability analysis of fractional order time delay systems. *Masinstvo*, 26(1):11–20, 2007.

[46] C. Fei, H. Li, and J. Yan. Finite-time stability of fractional-order neural networks with delay. *Neurocomputing*, 182:161–166, 2016.

[47] T. Abdeljawad and D. Baleanu. On fractional derivatives with exponential kernel and their discrete versions. *Reports on Mathematical Physics*, 84(3):367–378, 2019.

[48] I. M. Batiha, I. Bendib, A. Ouannas, I. H. Jebril, S. Alkhazaleh, and S. Momani. On new results of stability and synchronization in finite-time for fitzhugh-nagumo model using gronwall inequality and lyapunov function. *Journal of Robotics and Control (JRC)*, 5(6):1897–1909, Oct. 2024.

[49] I. Bendib, I. M. Batiha, A. Hioual, N. Anakira, M. Dalah, and A. Ouannas. On a new version of gierer-meinhardt model using fractional discrete calculus. *Results in Nonlinear Analysis*, 7(2):1–5, 2024.